Automatically Unrolling Decorations Painted on 3D Pottery

Ye Liu
School of Computer Software
Tianjin University

Bo Zhang
School of Computer Software
Tianjin University

Liang Wan*
School of Computer Software
Tianjin University
lwan@tju.edu.cn

ABSTRACT

Drawing pottery plays an important role in reporting archaeological findings. In addition to showing the form of a pot, it is essential to show decorations around the pot's body by means of 2D drawing. However, the traditional way of drawing pottery decorations in 2D plane involves intensive manual labors and rich specialist skills. For archaeological specialists, one major difficulty lies in manually unrolling pottery decorations from 3D surface to 2D plane with less distortions. In this paper, we address this problem by proposing an automatic method to unroll decorations on 3D pottery vessels into 2D planar space. As the first attempt to this problem, our approach considers the decoration appearance and utilizes geometry approximation to achieve piecewise unrolling. We validate our approach with different examples. As demonstrated in experimental results, our approach is simple to use, and is effective to generate unrolled 2D decorations.

CCS CONCEPTS

• **Computing methodologies** → **Texturing**; *Parametric curve and surface models*;

KEYWORDS

Decoration unrolling, pottery segmentation, conical frustum fitting

ACM Reference format:
Ye Liu, Bo Zhang, and Liang Wan. 2017. Automatically Unrolling Decorations Painted on 3D Pottery. In *Proceedings of CGI '17, Yokohama, Japan, June 27-30, 2017,* 6 pages.
DOI: 10.1145/3095140.3095177

1 INTRODUCTION

In recent decades, computer graphics technologies have been largely applied in the field of archaeology. A lot of effort has been put in 3D digitalization of cultural heritages, ranging from large-scale excavated sites to small-size mobile relics, like pottery. On the other hand, archaeological specialists utilize commercial image processing tools, including Adobe Illustrator or Photoshop, to facilitate archaeological drawing. Given a real pot or a scanned 3D pot model, drawing pottery is to show the form of the pot, its cross-section and decoration on the pot's body, in terms of 2D line drawings. However, the traditional way of drawing pottery decorations in 2D planar space involves intensive manual labors and rich specialist skills [10]. As illustrated in Figure 1, the decorations painted on the pot are to be piecewisely drawn in 2D space. In the traditional way, a specialist has to inspect the pot from surrounding different directions, and draws the line drawings as projected from orthographic views, such that the 2D drawings suffer less distortion. Mimicking the orthographic projection is not an easy task for human begins, which can be time consuming for even specialists.

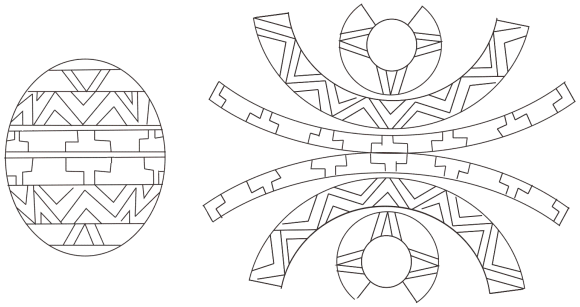

Figure 1: Illustration of archeological decoration drawing. Left: a line drawing of the front-view of a pottery. Right: the unrolled decorations in format of line drawing.

The process of drawing archaeological decoration inspires us to consider the interesting problem of automatically unrolling the decorations painted on 3D pottery into 2D planar space, obeying archaeological drawing rules. To the best of our knowledge, there is no academic publication reported on this problem. The most close work was reported in the recent news of the Metropolitan Museum of Art in New York [11], which has tried to unroll the captured 3D models of ceramic plates and cylindrical drinking vessels. However, the detailed technique of unrolling was not disclosed. Although given a 3D pottery model, graphics designers may apply UV mapping to help unrolling, manual adjustment is necessary. In this paper, we develop an automatic approach. Since the decorations painted on pottery can be treated as textures, our basic idea is approximating a 3D pot with a set of conical frustums, and then unrolling the frustum's surface into 2D space, which mimics the orthographic projection.

*Corresponding author

CGI '17, Yokohama, Japan

DOI: 10.1145/3095140.3095177

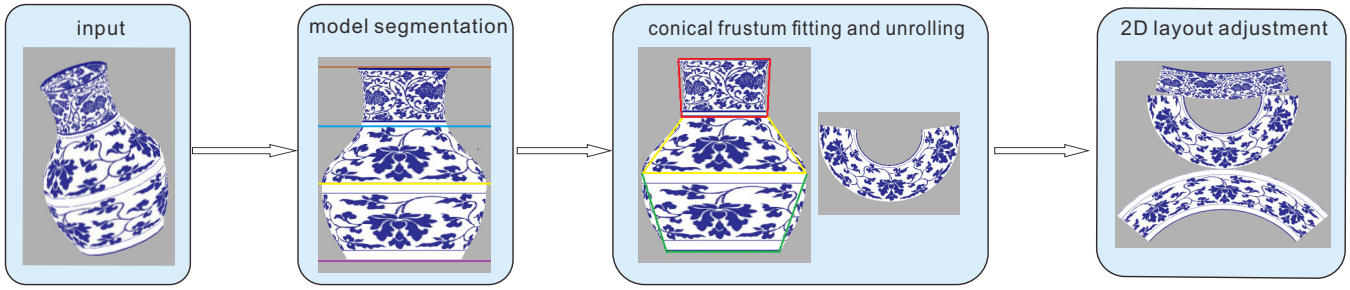

Figure 2: Our framework. Given a 3D pot, we segment it into portions with horizontal bases (the cutting planes are shown in different colors). Then each segment is fit with a conical frustum. In this example, three frustums are constructed (shown in different colors) and one frustum is unrolled for illustration. Finally the unrolled pattern is laid out in 2D planar space by adjusting the layout to avoid overlapping.

Specifically, we first segment the pot model into non-overlapped parts with parallel bases, by considering the decoration appearance. We then perform conical frustum fitting for each segmented part and unroll the approximated conical frustum into 2D space. Finally the unrolled textures are laid out in 2D space to obtain a pleasant unrolled result. By this way, we accomplish the piecewise unrolling by taking into considerations of both decoration appearance and geometry characteristics. Moreover, interactive merging control is provided in the system to further facilitate user operation. We validate our approach with different examples. As demonstrated in experimental results, our approach is simple to use and is effective to generate pleasant unrolled 2D decorations.

2 RELATED WORK

2.1 Surface Parameterization

Parameterization of geometric surfaces can be viewed as a one-to-one mapping from a surface to a suitable parameter domain [4]. As the parametrization is highly related to the underlying geometry of the surface, the existing methods can be roughly divided into two categories: 1) a direct mapping of coordinates from one geometry surface to the other; 2) using an auxiliary surface or geometric solid as an intermediate parameterization [6].

In general cases, there is no perfect way to map a surface to another without introducing some kinds of distortion, for example, in terms of angles, areas, and lengths. Desbrun et al. [3] defines the distortion as a combination of different intrinsic measures of the surface. Many previous works have been developed to minimize distortions in different ways. Gu and Yau [5] find a basis of the solution space from which all the parameteizations can be constructed. Hu et al. [7] develop a feature-aligned surface parameterization algorithm with the help of the SLO eigenfunctions and Loop subdivision basis functions. Liao et al. [8] propose a structure-aligned approach for surface parameterization using eigenfunctions from the Laplace-Beltrami operator. Smith and Schaefer [15] generate guaranteed bijective surface parameterizations from triangulated 3D surfaces, by using a distortion metric that prevents local folds of triangles in the parameterization and a barrier function that prevents intersection of the chart boundaries. In our work, we follow the archeologists' rules of drawing pottery decorations, using conical frustum as the intermediate paratemerization surface.

2.2 Conical Frustum Approximation

In the literature, many researchers have investigated the problem of computing the smallest enclosing cylinder (or cylindrical segment) for a set of 3D points [14] [2] [19]. Using cylinder only to fit the 3D model, like the pottery we deal with, may lead to obvious approximation errors. A more effective way is fitting 3D model with conical frustum.

To fit quadric surface such as cylinder and cone, Lukas et al. [9] propose a simplified distance measure to approximate the distance between the point cloud data and the model surface. Pratt [13] applies the quasi-least-squares method to do the fitting. An and Guan's method [1] is able to suppress noise in fitting point cloud data with cylinder and cone. Sun et al. [16] propose a method to divide the points into subsets, and approximate each subset with a conical frustum. Tempero et al. [18] project the points onto four side views and estimates the conical frustum based on the 2D convex hull of projected points. In our work, we approximate conical frustums by estimating the radius for the top and bottom circular bases.

3 AUTOMATIC DECORATION UNROLLING

3.1 Overview

By observing ancient pottery vessels, as demonstrated in Figure 3, we can get two interesting findings: 1) most pottery vessels are rotational symmetric; 2) most decorative patterns painted on pottery can be separated into portions with parallel bases. These may be because artificial objects, such as pottery, are made via rotation manufacturing process.

The textbook on archeological drawing [10] introduces the rules of drawing pottery decorations: if the pottery vessel is a simple geometry with developable surface (like a cone or a

Figure 3: Examples of pottery vessels.

cylinder), drawing decoration is similar to flatten the surface, which has no distortion; if the vessel is a geometry with non-developable surface, drawing decoration can be achieved by approximating the geometry with a cone or cylinder.

Following the two findings and the drawing rules, we develop an effective framework for automatic decoration unrolling. As illustrated in Figure 2, our framework contains three main steps: model segmentation which segments the pot into portions with parallel bases, conical frustum fitting and unrolling which maps each segment's texture to 2D space, and planar layout adjustment which generates a pleasant unrolled result.

3.2 Model Segmentation

As most decorative patterns on pottery can be separated into portions with parallel bases, we consider to segment the model according to the pattern's appearance. To ease the segmentation, we first estimate the symmetry axis using the method proposed in [17], then rotate the model to ensure its rotation symmetry axis coincident with the perpendicular axis of the coordinate system. In this way, the segmentation is converted to finding horizontal cutting lines in the orthographic side views of the pot model.

Here, we rely on gradient distribution to estimate the cutting lines (illustrated in Figure 4). We first render 4 side view images with 90-degree field-of-view via orthogonal projection, i.e. left, right, front and back side views. For each side view, we compute the horizontal gradients using the Sobel gradient operator, and sum the absolute values along the horizontal direction. After obtaining the summed gradient curve, the cutting lines correspond to the positions that have values close to zero and neighbouring gradient values form strong jumps, which is formulated as

$$L_c = \left\{ L_i \mid (G_{l_{i-1}} - \varepsilon)(G_{l_{i+1}} - \varepsilon) < 0 \right\}, \qquad (1)$$

where L_i denotes the i-th row, G_{l_i} denotes the gradient of i-th row, ε is the predefined threshold, and L_c denotes the cutting line. Thanks to the orthographic projection, we can easily locate the cutting planes in the 3D space from the detected cutting lines. With the cutting planes, the pot model

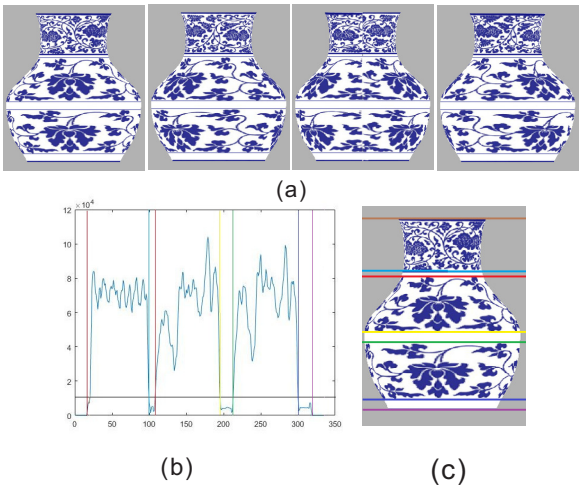

Figure 4: Model segmentation by locating the cutting planes. (a) shows four side views of the 3D model. (b) is the summed gradient cruve, in which the horizontal line represents the per-defined threshold, vertical lines are the detected cutting lines. (c) shows the cutting planes in 3D space.

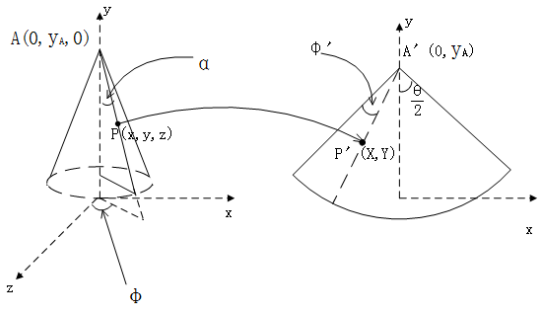

Figure 5: Unroll a cone to the planar space.

can be segmented into a set of 3D portions along the vertical direction, and each portion has some decoration pattern.

3.3 Conical Frustum Fitting and Unrolling

Given a segment, we now approximate the segment with a conical frustum. As the vessel is rotational symmetric, we can do the approximation by simply taking the top and bottom bases of the segment as circles, and estimating the radii and the height of the segment.

As illustrated in Figure 5, the unrolling of the fitted frustum is to transform each vertex $P(x, y, z)$ of the fitted conical frustum to a planar vertex $P'(X, Y)$. Let the corresponding cone of the fitted conical frustum has a height H and bottom radius R. Using spherical coordinates, the coordinates of P can be expressed as

$$P = (r \sin\phi, y, r \cos\phi), \qquad (2)$$

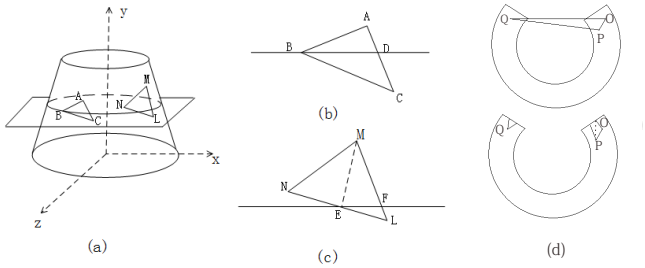

Figure 6: When (a) a cutting plane passes across triangles, the triangles are divided into smaller ones as in (b) and (c). (d) shows a triangle passing across the boundary of the flattened frustum.

where $r = \frac{h}{H}R$ is the distance from P to y-axis, and $h = y_A - y$, the azimuth angle ϕ is computed by $\phi = \arccos \frac{z}{\sqrt{x^2+z^2}}$. The unrolling depends on the choice of the vertical cut, which is set in the positive z direction. With some mathematics, we can deduce the formula to calculate $P'(X, Y)$:

$$\begin{cases} X = \sqrt{h^2 + r^2} sin(\frac{\theta}{2} - \phi'), \\ Y = y_A - \sqrt{h^2 + r^2} cos(\frac{\theta}{2} - \phi'), \end{cases} \tag{3}$$

where

$$\begin{cases} \phi' = \frac{r}{\sqrt{h^2 + r^2}} \arccos \frac{z}{\sqrt{x^2 + z^2}}, \\ \frac{\theta}{2} = \frac{\pi R}{\sqrt{H^2 + R^2}}. \end{cases} \tag{4}$$

It's worth noting that the above equation assumes x is positive. When x is negative, the angle ϕ' is

$$\phi' = \frac{r}{\sqrt{h^2 + r^2}} (\arccos(-1) \frac{z}{\sqrt{x^2 + z^2}} + \pi). \tag{5}$$

Note that a 3D pot model is usually represented as a triangular mesh. In the unrolling, there are some special cases that deserve considerations. As illustrated in Figure 6(a), some triangles may be cut through by the cutting planes. To tackle this situation, we need to decompose one such triangle into several smaller triangles. As shown in Figure 6(b), a triangle is decomposed into two small triangles when the cutting plane passes by one triangle vertex. When the cutting plane passes across two triangle edges, the triangle is decomposed into three smaller triangles (Figure 6(c)). On the other hand, the unrolling may cause some triangles pass across the boundary of the flattened frustum (illustrated in Figure 6(d)). Similarly, we also divide such triangles into smaller ones.

3.4 2D Layout Adjustment

After unrolling, overlapping between unrolled fragments may occur, as shown in Figure 7(a). To handle this problem, we adjust the layout in 2D space. In more detail, we keep the bottom fragment as the baseline and move the other fragments upwards until they have no intersections. From Figure 7(b), we can clearly see that the intersections between unrolled fragments are removed effectively after layout adjustment, and the result is more plausible.

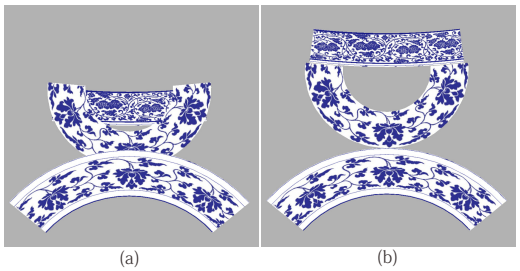

Figure 7: Adjust the layout of the unrolled decoration segments to avoid overlaps: (a) before adjustment; (b) after adjustment.

Figure 8: Automatic unrolling effects. (a) is the input 3D model. (b) and (c) are unrolling results without/with less-textured segment merging.

By observing pottery decorations, we notice that there may exist less-textured segments, and they may affect the visual effect of the unrolling decoration (Figure 8(b)). For this case, we can merge such a segment with one of its neighbours. An automatic way is to select the neighbour such that they have close mean values of their top and bottom radii, given by

$$C_i' = \begin{cases} C_{i+1}, & \text{If } |R_i - R_{i+1}| < |R_i - R_{i-1}|, \\ C_{i-1}, & \text{others.} \end{cases} \tag{6}$$

where R_i is the mean radius of one fitted conical frustum C_i. After the merging, one cutting plane will be removed, and then we reconduct conical frustum fitting and unrolling for the merged segments. Figure 8(c) shows one example after the less-textured segment merging.

4 EXPERIMENTAL RESULTS

To validate our algorithm, we collect several vessel models which have different geometric forms and different decorations painted on the pots' bodies. The pot models tested in our experiments are acquired in two ways: 1) downloaded from the online 3D model website [12] (Figures 9, 11(a), 11(c)); 2) created manually using 3ds Max (Figures 4, 8, 11(b)).

In this following, we first show effects from applying automatic unrolling and interactive unrolling, then make comparison with unrolling using cylinder approximation, and finally report the timing performance.

4.1 Effects from Automatic Unrolling

In Figure 8(a), we show a 3D vassel model with 600 vertices and 1,140 triangles, and its summed gradient distribution of

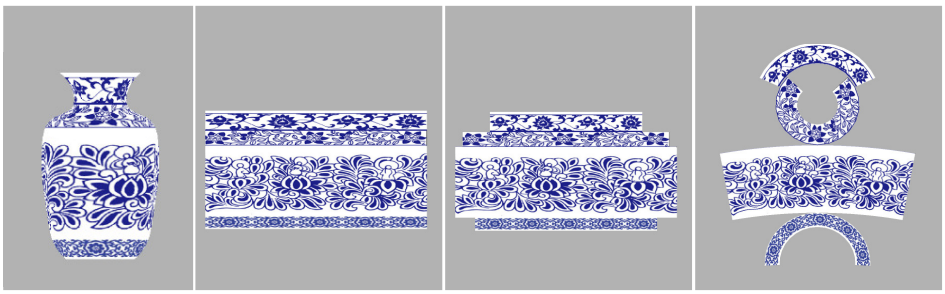

Figure 10: Comparison with unrolling using cylinder fitting: (a) the 3D model, (b) the result from cylinder unrolling, (c) the result from piecewise cylinder unrolling, and (d) the result from our method.

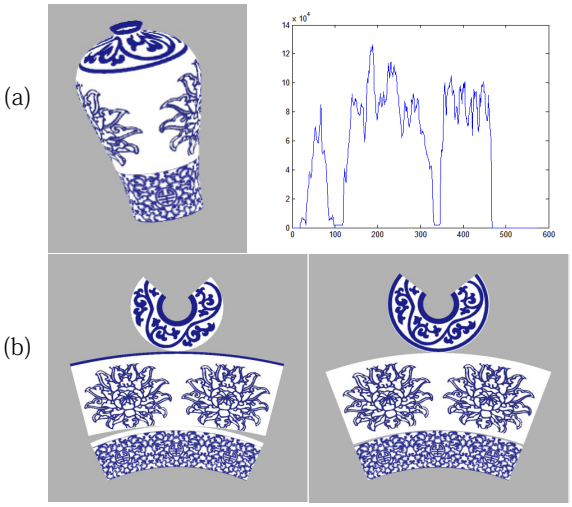

Figure 9: Results with interactive merging control: (a) the input 3D model and the summed gradient curve, (b) the unrolled result from automatic unrolling and that with interactive merging control.

side views. We can clearly see that the summed gradients have obvious small values at certain positions. As shown in Figure 8(b), our segmentation produces reasonable cutting planes. We also note that there is a nearly white segment near the centre. By performing automatic less-textured segment merging, the white segment is merged to the segment below it (Figure 8(c)), and the unrolled result is updated accordingly.

The unrolling results shown in Figures 8(b) and (c) both look plausible. They can be used as reference to help archeologists to produce decoration line drawings.

4.2 Effects with Interactive Merging Control

To further facilitate user intervention and provide more flexibility, we provide interactive merging control in our system. Users can select and merge two neighbouring segments in an interactive manner.

Figure 9 shows a 3D vassel model with 1,024 vertices and 1,984 triangles, the unrolled result from automatic unrolling, and the unrolled result with interactive merging control. As we can observe from the left result in Figure 9(b), the decoration unrolling near the bottom is not so satisfied, since our current less-textured segment merging only considers geometry property only. As shown in the right result in Figure 9(b), a more pleasant result can be achieved by tuning the merging manually.

4.3 Comparison with Unrolling using Cylinder Fitting

Since decoration unrolling is a new problem, there are no existing methods for this problem. Here, we make comparison with two alternative solutions. The first is replacing conical frustum with cylinder in our framework, named as piecewise cylinder unrolling. The second is fitting the whole model with one cylinder solely, named as cylinder unrolling.

The comparison results are shown in Figure 10. From the figure, we can see that the three methods have similar unrolled results in the middle part, which is close to a cylinder. When approximating the whole model with one cylinder solely, the texture of the top segment with small radius is stretched seriously (Figure 10(b)). This problem is alleviated for piecewise cylinder unrolling. However, for the second top segment, piecewise cylinder unrolling still suffers from obvious stretching, as compared to the 3D model. Our result, on the other hand, has much less distortion and the shape of unrolled segments can indicate the form of the 3D model.

4.4 More Results

Figure 11 shows unrolled results for more 3D pottery vessels. It is obvious that our approach is able to segment 3D models reasonably. By applying our automatic unrolling, we can get reasonable unrolled decorations for most vessels (see the second and third examples). With interactive merging control, we can also easily adjust the unrolled results to get satisfied results (see the first example).

4.5 Timing Performance

In the end, we report running times of our algorithm in Table 1. Our system is implemented using C++ on a machine installed with Intel(R) Core(TM) i5-3330 CPU@3.00GHz

with 16GB RAM. As evidenced in Table 1, we can see that the running time grows with the number of vertices and triangles. In general, our system is rather fast and able to achieve interactive performance.

Table 1: Timing performance of automatic decoration unrolling.

Model	Vertex number	Triangle number	Time (s)
Fig 2	640	1,248	0.250
Fig 8	600	1,140	0.256
Fig 9	1,024	1,984	0.312
Fig 11(a)	1,584	3,072	0.499
Fig 11(b)	928	1,824	0.593
Fig 11(c)	44,000	87,599	22.511

5 CONCLUSIONS

In this paper, inspired by archeological decoration drawings, we address an interesting problem of unrolling the decorations painted on 3D pottery into 2D planar space. Following the drawing rules used in archeological drawing, we propose a simple and effective approach. We first segment the 3D model along its symmetric axis by conducting segmentation in the side-view image space. Then each segment is further fitted as a conical frustum and undergoes the unrolling. Finally, we adjust the layout of the unrolled segment to obtain a pleasant unrolled result.

In our current work, we only process pots without handles. In the future, we want to study how to deal with a vessel with handlers sticking outside of the vessel. In addition, we would like to collect some scanned 3D models of pottery vessels, and apply our method on real data.

6 ACKNOWLEDGEMENTS

This work is supported by the National Natural Science Foundation of China (61572354), and the National Science and Technology Support Project (2014BAK09B04).

Figure 11: More results. From left to right are 3D models, results from automatic unrolling, and results with interactive segment merging.

REFERENCES

[1] L. I. An and Ai Zhi Guan. 2007. Fitting Point Cloud to Cone and Cylinder Based on Gaussian Image. *Modular Machine Tool & Automatic Manufacturing Technique* (2007).
[2] Timothy M Chan. 2011. Approximating the diameter, width, smallest enclosing cylinder, and minimum-width annulus. In *Sixteenth Symposium on Computational Geometry*. 300–309.
[3] Mathieu Desbrun, Mark Meyer, and Pierre Alliez. 2002. Intrinsic Parameterizations of Surface Meshes. *Computer Graphics Forum* 21, 3 (2002), 209–218.
[4] Michael S. Floater and Hormann Kai. 2005. Surface Parameterization: a Tutorial and Survey. 1 (2005), 157–186.
[5] Xianfeng Gu and Shing Tung Yau. 2003. Global conformal surface parameterization. In *Eurographics/acm SIGGRAPH Symposium on Geometry Processing*. 127–137.
[6] Steven Haker, Sigurd Angenent, Allen Tannenbaum, Ron Kikinis, Guillermo Sapiro, and Michael Halle. 2000. Conformal surface parameterization for texture mapping. *IEEE Transactions on Visualization & Computer Graphics* 6, 2 (2000), 181 – 189.
[7] Kangkang Hu, Yongjie Jessica Zhang, Xinge Li, and Guoliang Xu. 2016. Feature-aligned Surface Parameterization Using Secondary Laplace Operator and Loop Subdivision. *Procedia Engineering* 163 (2016), 186–198.
[8] Tao Liao, Guoliang Xu, and Yongjie Jessica Zhang. 2014. Structure-aligned guidance estimation in surface parameterization using eigenfunction-based cross field. *Graphical Models* 76, 6 (2014), 691–705.
[9] Gabor Lukcs, Ralph Martin, and Dave Marshall. 1998. Faithful Least-Squares Fitting of Spheres, Cylinders, Cones and Tori for Reliable Segmentation. In *Computer Vision - Eccv'98, European Conference on Computer Vision, Freiburg, Germany, June 2-6, 1998, Proceedings, Volume I*. 671–686.
[10] Hongzao Ma. 2008. *Archaeological drawing*. Peking University Press.
[11] The Metropolitan Museum of Art. 2016. sketchfab. http://www.metmuseum.org/blogs/now-at-the-met/2016/unrolling-maya-ceramic-canvases. (2016).
[12] Cedric Pinson. 2012. sketchfab. https://sketchfab.com/. (2012).
[13] Vaughan Pratt. 2002. Direct least-squares fitting of algebraic surfaces. *Acm Siggraph Computer Graphics* 21, 4 (2002), 145–152.
[14] Elmar Schömer, Jrgen Sellen, Marek Teichmann, and Chee Yap. 2000. Smallest enclosing cylinders. *Algorithmica* 27, 2 (2000), 170–186.
[15] Jason Smith and Scott Schaefer. 2015. Bijective parameterization with free boundaries. *Acm Transactions on Graphics* 34, 4 (2015), 1–9.
[16] Chunjuan Sun, Binha Zhu, and Wenchengi Wang. 2010. Optimizing Conical Reconstruction of Linear Point Clouds. *Journal of Computer-Aided Design & Computer Graphics* 22, 8 (2010), 1324–1330.
[17] Andrea Tagliasacchi, Hao Zhang, and Daniel Cohen-Or. 2009. Curve skeleton extraction from incomplete point cloud. *Acm Transactions on Graphics* 28, 3 (2009), 341–352.
[18] Russell Tempero, Sergey Bereg, Xiangxu Meng, Changhe Tu, Chenglei Yang, and Binhai Zhu. 2008. Automatically Approximating 3D Points with Co-Axisal Objects. In *International Conference on Computational Sciences and ITS Applications*. 373–381.
[19] Binhai Zhu. 2011. Approximating 3D Points with Cylindrical Segments. In *International Conference on Computing and Combinatorics*. 420–429.